CLICdp-Note-2018-002
26 November 2018

Updated CLIC luminosity staging baseline and Higgs coupling prospects

A. Robson[1)*], P. Roloff[†]

[*] *University of Glasgow, United Kingdom,* [†] *CERN, Geneva, Switzerland*

Abstract

An updated luminosity staging baseline for CLIC is presented. Assuming accelerator ramp-up and up-time scenarios that are harmonized with those of other potential future colliders, CLIC will deliver $1\,\text{ab}^{-1}$ at $\sqrt{s} = 380\,\text{GeV}$, $2.5\,\text{ab}^{-1}$ at $\sqrt{s} = 1.5\,\text{TeV}$, and $5\,\text{ab}^{-1}$ at $\sqrt{s} = 3\,\text{TeV}$. The complete programme will take 25–30 years. The baseline scenario for luminosity sharing between the two electron beam polarisation states is also discussed. Updated Higgs coupling sensitivities are given for this new luminosity staging baseline.

[1] Also at CERN, Geneva, Switzerland

1 Introduction

CLIC offers high-energy e^+e^- collisions up to centre-of-mass energies of 3 TeV [1]. A rich programme of Higgs and top-quark physics is uniquely provided by the initial energy stage around $\sqrt{s} = 380\,\text{GeV}$; this is supplemented at the higher-energy stages by increased precision in Higgs and top-quark physics, and further reach to beyond-Standard Model (BSM) effects.

The revised luminosity baseline comes in the context of an initiative to harmonize the assumptions used by several future collider projects [2], and presents an opportunity to reassess the optimal staging scenario for physics reach in light of recent studies. The effect of harmonizing the collider up-time and ramp-up assumptions, as well as modest adjustments to the time spent at each CLIC energy stage, is to increase substantially the integrated luminosity that is foreseen for CLIC.

The updated running assumptions and resulting integrated luminosities are described in section 2 of this note. A baseline polarisation scenario is given in section 3, and the resulting Higgs coupling sensitivities are discussed in section 4.

2 Staging

In the revised scenario, the assumed run period per year is 185 days. This allows for a long shutdown of around 120 days per year; start-up of around 30 days; and longer machine development and technical stops of around 30 days. The assumption of 75% efficiency during the 185-day run period, to allow for faults and preventative maintenance, results in a running time of 1.2×10^7 s per year. This is based on previous CERN experience and has been agreed with the FCC projects as a common baseline. It is less than the ILC scenario, which assumes running for 1.6×10^7 s per year (computed as 75% of 8 months, i.e. running for 185 days) [3]. However, it is more than what was foreseen in the previous CLIC baseline, which assumed a running time of 1.08×10^7 s per year [4].

At the initial energy stage, $\sqrt{s} = 380\,\text{GeV}$, the accelerator is expected to ramp up to its nominal performance over the first three years of running. In this revised baseline, the delivered luminosity is assumed to be 10%, 30%, and 60% of the nominal luminosity in each of these ramp-up years, respectively. This ramp-up scenario matches that assumed by the ILC. The three-year ramp-up period will be followed by five years running at the nominal luminosity, to deliver a total integrated luminosity of $1\,\text{ab}^{-1}$. This includes $100\,\text{fb}^{-1}$ taken in an energy scan around the $\text{t}\bar{\text{t}}$ production threshold.

For the subsequent energy stages, 1.5 TeV and 3 TeV, the accelerator is expected to reach its nominal performance after two years, and a ramp-up of 25% and 75% of the nominal luminosity in the first two years of each stage is assumed. This also matches the ILC scenario.

At $\sqrt{s} = 1.5\,\text{TeV}$, the ramp-up will be followed by five years of running at the nominal luminosity, yielding a total integrated luminosity of $2.5\,\text{ab}^{-1}$. At $\sqrt{s} = 3\,\text{TeV}$, the ramp-up will be followed by six years of running at the nominal luminosity, for a total integrated luminosity of $5\,\text{ab}^{-1}$.

At each stage the collider is run for slightly longer in the revised scenario, compared with the previous scenario [4]. Running for longer at each stage, when the collider has reached its nominal luminosity, both takes advantage of the machine's full design performance, and is more consistent with the cost and time requirements of staging the machine's construction.

The total integrated luminosities are summarized in Table 1. The ramp-up scenario is shown as luminosity per year in Figure 1 and total integrated luminosity in Figure 2.

3 Polarisation

The CLIC baseline has $\pm 80\%$ longitudinal polarisation for the electron beam, and no positron polarisation. At the initial energy stage, the dominant Higgs production cross section is Higgsstrahlung, which is not much affected by the electron polarisation. Collecting data from both polarisations improves the

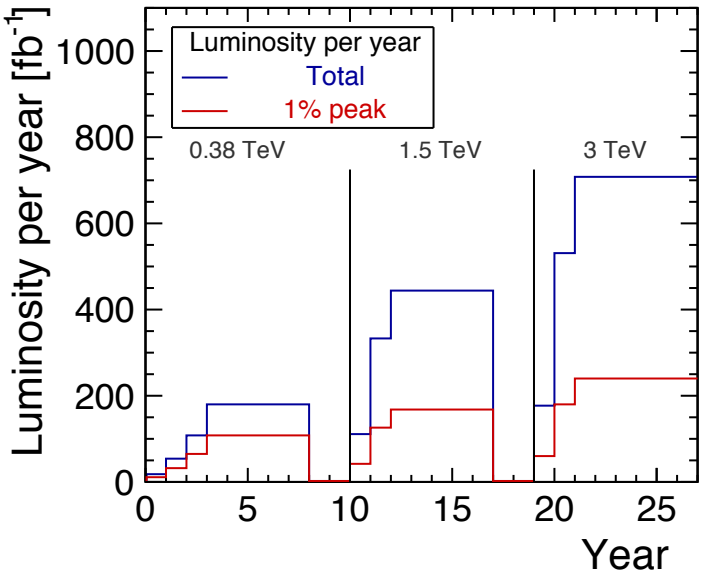

Figure 1: Luminosity per year in the updated CLIC staging scenario. For the first stage the luminosity ramp-up is three years (10%, 30%, 60%) and for the subsequent stages two years (25%, 75%). As a result of beamstrahlung the CLIC beam spectrum has a low-energy tail, so both the total luminosity per year, and the luminosity collected above 99% of the nominal $\sqrt{s}$ (labelled '1% peak'), are shown.

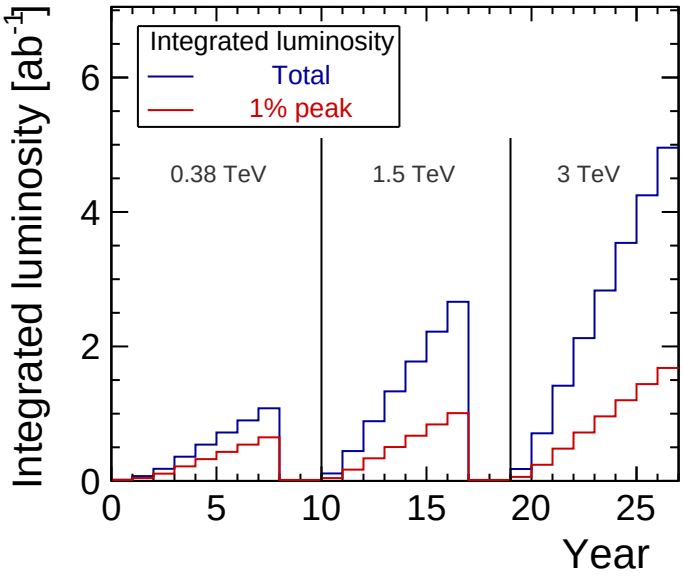

Figure 2: Integrated luminosity in the updated CLIC staging scenario. The luminosity ramp-up corresponds to what is described in Figure 1.

Stage	$\sqrt{s}$ [TeV]	$\mathscr{L}_{int}$ [ab^{-1}]	$P(e^-)$=–80% $\mathscr{L}_{int}$ [ab^{-1}]	$P(e^-)$=+80% $\mathscr{L}_{int}$ [ab^{-1}]
1	0.38 (and 0.35)	1.0	0.5	0.5
2	1.5	2.5	2.0	0.5
3	3.0	5.0	4.0	1.0

Table 1: Baseline CLIC energy stages and integrated luminosities for each stage in the updated scenario.

sensitivity to certain BSM effects, for example in two-fermion production. Consequently, equal amounts of –80% and +80% polarisation running are foreseen at the initial energy stage. At the higher-energy stages, the dominant Higgs production mechanism is through WW fusion, and double-Higgs production becomes accessible. Single and double-Higgs production through WW-fusion is significantly enhanced by around 80% by running with –80% electron polarisation, while it is reduced by the same amount with +80% polarisation [5]. However, some +80% electron polarisation running is required for sensitivity to certain BSM effects. For the two higher-energy stages, a baseline is adopted of sharing the running time for –80% and +80% electron polarisation in the ratio 80:20.

4 Higgs couplings

One of the unique capabilities of lepton colliders is to measure the total production cross section for the Higgsstrahlung process, $\sigma(\mathrm{ZH})$, using only the system that recoils against the produced Higgs boson and without examining the Higgs decay products. In turn, this allows the Higgs couplings to be extracted in a model-independent way (for example, without including any assumption about the absence of BSM invisible decays of the Higgs boson) from the cross sections times branching ratios of individual final states. The uncertainty of the measured $\sigma(\mathrm{ZH})$ therefore contributes to the precision of all of the other Higgs coupling measurements. This recoil measurement is only possible at the initial CLIC energy stage, and obtaining a high-accuracy measurement of $\sigma(\mathrm{ZH})$ is a main motivation for planning a relatively long run at $\sqrt{s} = 380\,\mathrm{GeV}$.

At the highest energy stage, several flagship measurements such as double Higgs boson production are limited by statistics, providing a motivation for increased luminosity also at the higher energies.

4.1 Summary of Higgs observables

Extensive studies of the CLIC sensitivities to Higgs couplings have been reported previously in [5]. Details of the analyses and combined fitting can be found there. For those studies, an earlier energy staging of $\sqrt{s} = 350\,\mathrm{GeV}$, 1.4 TeV, and 3 TeV was assumed, with corresponding integrated luminosities of 0.5, 1.5, and 3 ab^{-1}. As a consequence of those and other studies, the present initial stage energy of $\sqrt{s} = 380\,\mathrm{GeV}$ was adopted in order to optimise the physics reach of the initial stage by including precise measurements of top-quark properties above threshold. In this document, the precisions of the individual Higgs sector measurements are updated for the integrated luminosities of the present staging scenario: 1.0, 2.5, and 5.0 ab^{-1}, and for the polarisation baseline scenario, while still using the previous energy stages.

Precisions on the Higgs observables are given in Table 2 for the first energy stage, and in Table 3 for the two higher-energy stages. These individual results assume unpolarised beams.

Measurement of the cross section for double-Higgs production at 1.4 and 3 TeV gives sensitivity to the Higgs self-coupling λ. Assuming unpolarised beams, the precision on $\sigma(\mathrm{HH}\nu_e\bar{\nu}_e)$ that comes from 2.5 ab^{-1} of integrated luminosity at 1.4 TeV results in a statistical precision on λ of 42%, which reduces

to 18% with 5.0 ab^{-1} at 3 TeV. Assuming −80% electron polarisation, these precisions improve to 31% and 14%, respectively. The additional inclusion of differential measurements at 3 TeV, and the ZHH double-Higgsstrahlung cross section at 1.4 TeV, yields a precision of $[-7\%, +11\%]$ on λ.

The recoil mass analysis from $e^+e^- \to ZH$ events can be used to search for BSM decay modes of the Higgs boson into 'invisible' final states. Scaling the result from [5] to the updated luminosity staging scenario gives an upper limit on the invisible Higgs branching ratio of BR(H → invis.) < 0.69% at 90% C.L. in the modified frequentist approach (for 1 ab^{-1} at $\sqrt{s} = 350$ GeV).

Channel	Measurement	Observable	Statistical precision 350 GeV 1 ab^{-1}	Reference [5]
ZH	Recoil mass distribution	m_H	78 MeV	[5]
ZH	$\sigma(ZH) \times BR(H \to \text{invisible})$	Γ_{inv}	0.4 %	[5]
ZH	$\sigma(ZH) \times BR(Z \to l^+l^-)$	g^2_{HZZ}	2.7 %	[5]
ZH	$\sigma(ZH) \times BR(Z \to q\bar{q})$	g^2_{HZZ}	1.3 %	[5]
ZH	$\sigma(ZH) \times BR(H \to b\bar{b})$	$g^2_{HZZ}g^2_{Hbb}/\Gamma_H$	0.61 %	[5]
ZH	$\sigma(ZH) \times BR(H \to c\bar{c})$	$g^2_{HZZ}g^2_{Hcc}/\Gamma_H$	10 %	[5]
ZH	$\sigma(ZH) \times BR(H \to gg)$		4.3 %	[5]
ZH	$\sigma(ZH) \times BR(H \to \tau^+\tau^-)$	$g^2_{HZZ}g^2_{H\tau\tau}/\Gamma_H$	4.4 %	[5]
ZH	$\sigma(ZH) \times BR(H \to WW^*)$	$g^2_{HZZ}g^2_{HWW}/\Gamma_H$	3.6 %	[5]
$H\nu_e\bar{\nu}_e$	$\sigma(H\nu_e\bar{\nu}_e) \times BR(H \to b\bar{b})$	$g^2_{HWW}g^2_{Hbb}/\Gamma_H$	1.3 %	[5]
$H\nu_e\bar{\nu}_e$	$\sigma(H\nu_e\bar{\nu}_e) \times BR(H \to c\bar{c})$	$g^2_{HWW}g^2_{Hcc}/\Gamma_H$	18 %	[5]
$H\nu_e\bar{\nu}_e$	$\sigma(H\nu_e\bar{\nu}_e) \times BR(H \to gg)$		7.2 %	[5]

Table 2: Summary of the precisions obtainable for the Higgs observables in the first stage of CLIC for an integrated luminosity of 1 ab^{-1} at $\sqrt{s} = 350$ GeV, assuming unpolarised beams. For the branching ratios, the measurement precision refers to the expected statistical uncertainty on the product of the relevant cross section and branching ratio; this is equivalent to the expected statistical uncertainty of the product of couplings divided by Γ_H as indicated in the third column.

4.2 Combined fits

Precisions on the Higgs couplings and width extracted from a model-independent global fit, described in [5], are given in Table 4 and Figure 3. The fit assumes the present baseline scenario for integrated luminosities and beam polarisation. The increase in cross section from having a predominantly negatively-polarised electron beam is taken into account by multiplying the event rates for all WW-fusion measurements by a factor of 1.48, corresponding to a factor of 1.8 for 80 % of the statistics and 0.2 for the remaining 20 %. This approach is conservative because it assumes that all backgrounds, including those from *s*-channel processes, which do not receive the same polarisation enhancement, scale by the same amount.

Each energy stage contributes significantly to the Higgs programme: the initial stage provides g_{HZZ} and couplings to most fermions and bosons, while the higher-energy stages improve them and add the top-quark, muon, and photon couplings. The precision on g_{HZZ} is determined by the statistics at the initial stage.

The final precision of the model-independent couplings are shown as a function of particle mass in Figure 5. Precisions extracted from a model-dependent global fit, also described in [5], are given in

Channel	Measurement	Observable	Statistical precision 1.4 TeV 2.5 ab^{-1}	Statistical precision 3 TeV 5.0 ab^{-1}	Reference
$H\nu_e\bar{\nu}_e$	$H \to b\bar{b}$ mass distribution	m_H	36 MeV	28 MeV	[5]
ZH	$\sigma(ZH) \times BR(H \to b\bar{b})$	$g^2_{HZZ}g^2_{Hbb}/\Gamma_H$	2.6 %†	4.3 %†	[6]
$H\nu_e\bar{\nu}_e$	$\sigma(H\nu_e\bar{\nu}_e) \times BR(H \to b\bar{b})$	$g^2_{HWW}g^2_{Hbb}/\Gamma_H$	0.3 %	0.2 %	[5]
$H\nu_e\bar{\nu}_e$	$\sigma(H\nu_e\bar{\nu}_e) \times BR(H \to c\bar{c})$	$g^2_{HWW}g^2_{Hcc}/\Gamma_H$	4.7 %	4.4 %	[5]
$H\nu_e\bar{\nu}_e$	$\sigma(H\nu_e\bar{\nu}_e) \times BR(H \to gg)$		3.9 %	2.7 %	[5]
$H\nu_e\bar{\nu}_e$	$\sigma(H\nu_e\bar{\nu}_e) \times BR(H \to \tau^+\tau^-)$	$g^2_{HWW}g^2_{H\tau\tau}/\Gamma_H$	3.3 %	2.8 %	[5]
$H\nu_e\bar{\nu}_e$	$\sigma(H\nu_e\bar{\nu}_e) \times BR(H \to \mu^+\mu^-)$	$g^2_{HWW}g^2_{H\mu\mu}/\Gamma_H$	29 %	16 %	[5]
$H\nu_e\bar{\nu}_e$	$\sigma(H\nu_e\bar{\nu}_e) \times BR(H \to \gamma\gamma)$		12 %	6 %*	[5]
$H\nu_e\bar{\nu}_e$	$\sigma(H\nu_e\bar{\nu}_e) \times BR(H \to Z\gamma)$		33 %	19 %*	[5]
$H\nu_e\bar{\nu}_e$	$\sigma(H\nu_e\bar{\nu}_e) \times BR(H \to WW^*)$	g^4_{HWW}/Γ_H	0.8 %	0.4 %*	[5]
$H\nu_e\bar{\nu}_e$	$\sigma(H\nu_e\bar{\nu}_e) \times BR(H \to ZZ^*)$	$g^2_{HWW}g^2_{HZZ}/\Gamma_H$	4.3 %	2.5 %*	[5]
He^+e^-	$\sigma(He^+e^-) \times BR(H \to b\bar{b})$	$g^2_{HZZ}g^2_{Hbb}/\Gamma_H$	1.4 %	1.5 %*	[5]
$t\bar{t}H$	$\sigma(t\bar{t}H) \times BR(H \to b\bar{b})$	$g^2_{Htt}g^2_{Hbb}/\Gamma_H$	5.7 %	–	[7]

Table 3: Summary of the precisions obtainable for the Higgs observables in the higher-energy CLIC stages for integrated luminosities of 2.5 ab^{-1} at $\sqrt{s} = 1.4$ TeV, and 5.0 ab^{-1} at $\sqrt{s} = 3$ TeV. In both cases unpolarised beams have been assumed. For g_{Htt}, the 3 TeV case has not yet been studied. Numbers marked with $*$ are extrapolated from $\sqrt{s} = 1.4$ TeV to $\sqrt{s} = 3$ TeV while $\dagger$ indicates projections based on fast simulations. For the branching ratios, the measurement precision refers to the expected statistical uncertainty on the product of the relevant cross section and branching ratio; this is equivalent to the expected statistical uncertainty of the product of couplings divided by Γ_H, as indicated in the third column.

Table 5 and Figure 4. This fit also assumes the present baseline scenario for integrated luminosities and beam polarisation. Comparisons between the CLIC-only model-dependent Higgs coupling sensitivities and corresponding HL-LHC projections [8] are given in Figure 6, showing that already after the initial energy stage, in many cases the CLIC precision is significantly better than for the HL-LHC, and improves further with the higher-energy running.

5 Conclusions

The updated CLIC luminosity staging baseline assumes 1.0, 2.5, and 5.0 ab^{-1} collected at the three energy stages of $\sqrt{s} = 380$ GeV, 1.5 TeV, and 3 TeV, respectively.

A baseline polarisation scenario foresees running time for –80% and +80% electron polarisation shared equally at the initial energy stage, and shared in the ratio 80:20 for the two higher-energy stages.

Updated Higgs coupling sensitivities are presented for this new baseline scenario that show excellent precision at the percent level for many of the Higgs couplings from a model-independent fit, and precisions from a model-dependent fit that are in many cases significantly better than those projected for the HL-LHC.

Parameter	Relative precision		
	350 GeV $1\,\text{ab}^{-1}$	+ 1.4 TeV $+ 2.5\,\text{ab}^{-1}$	+ 3 TeV $+ 5\,\text{ab}^{-1}$
g_{HZZ}	0.6 %	0.6 %	0.6 %
g_{HWW}	1.0 %	0.6 %	0.6 %
g_{Hbb}	2.1 %	0.7 %	0.7 %
g_{Hcc}	4.4 %	1.9 %	1.4 %
$g_{\text{H}\tau\tau}$	3.1 %	1.4 %	1.0 %
$g_{\text{H}\mu\mu}$	–	12.1 %	5.7 %
g_{Htt}	–	3.0 %	3.0 %
$g^{\dagger}_{\text{Hgg}}$	2.6 %	1.4 %	1.0 %
$g^{\dagger}_{\text{H}\gamma\gamma}$	–	4.8 %	2.3 %
$g^{\dagger}_{\text{HZ}\gamma}$	–	13.3 %	6.7 %
Γ_{H}	4.7 %	2.6 %	2.5 %

Table 4

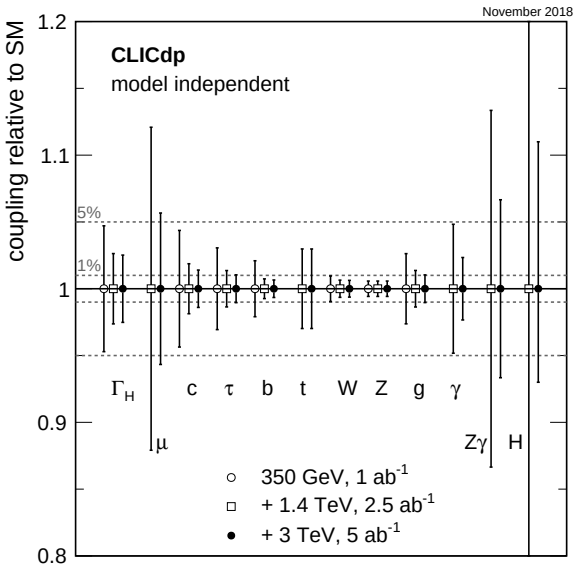

Figure 3

Results of the model-independent fit. For g_{Htt}, the 3 TeV case has not yet been studied. The three effective couplings $g^{\dagger}_{\text{Hgg}}$, $g^{\dagger}_{\text{H}\gamma\gamma}$ and $g^{\dagger}_{\text{HZ}\gamma}$ are also included in the fit. Operation with $-80\,\%$ ($+80\,\%$) electron beam polarisation is assumed for 80 % (20 %) of the collected luminosity above 1 TeV, corresponding to the baseline scenario.

Parameter	Relative precision		
	350 GeV $1\,\text{ab}^{-1}$	+ 1.4 TeV $+ 2.5\,\text{ab}^{-1}$	+ 3 TeV $+ 5\,\text{ab}^{-1}$
κ_{HZZ}	0.4 %	0.3 %	0.2 %
κ_{HWW}	0.8 %	0.2 %	0.1 %
κ_{Hbb}	1.3 %	0.3 %	0.2 %
κ_{Hcc}	4.1 %	1.8 %	1.3 %
$\kappa_{\text{H}\tau\tau}$	2.7 %	1.2 %	0.9 %
$\kappa_{\text{H}\mu\mu}$	–	12.1 %	5.6 %
κ_{Htt}	–	2.9 %	2.9 %
κ_{Hgg}	2.1 %	1.2 %	0.9 %
$\kappa_{\text{H}\gamma\gamma}$	–	4.8 %	2.3 %
$\kappa_{\text{HZ}\gamma}$	–	13.3 %	6.6 %

Table 5

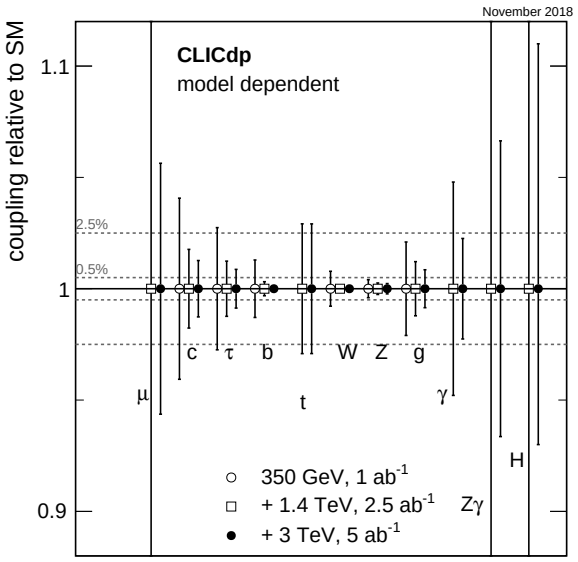

Figure 4

Results of the model-dependent fit without theoretical uncertainties. For κ_{Htt}, the 3 TeV case has not yet been studied. The uncertainty of the total width is calculated from the fit results. Operation with $-80\,\%$ ($+80\,\%$) electron beam polarisation is assumed for 80 % (20 %) of the collected luminosity above 1 TeV, corresponding to the baseline scenario.

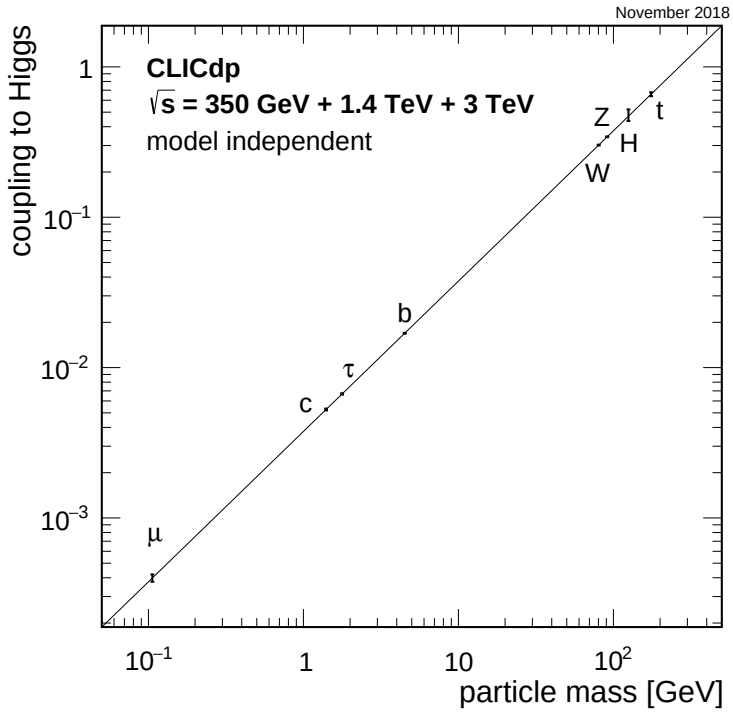

Figure 5: Precision of the model-independent Higgs couplings and the self-coupling as a function of particle mass. The line shows the SM prediction that the Higgs coupling of each particle is proportional to its mass.

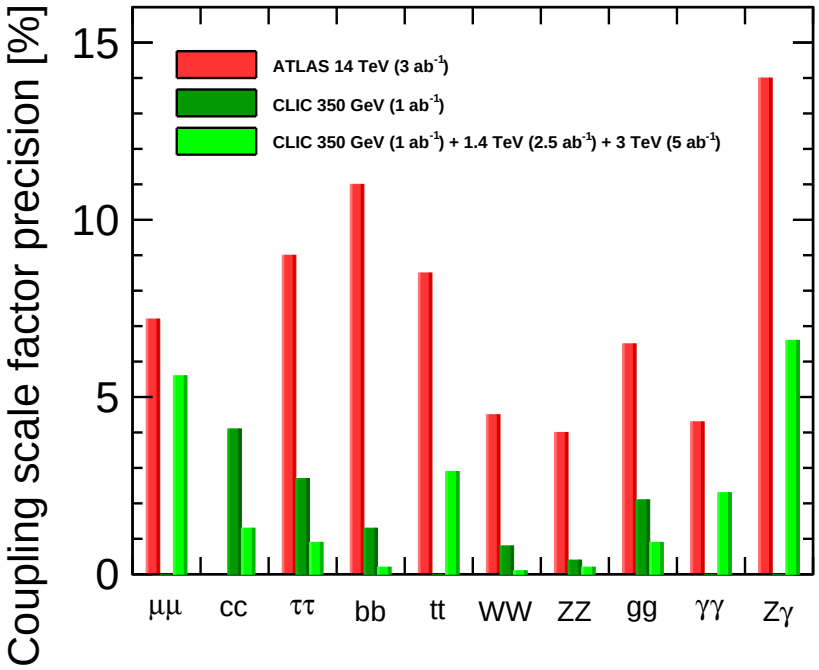

Figure 6: Comparison of the model-dependent Higgs couplings with projections [8] for HL-LHC.

References

[1] *Compact Linear Collider (CLIC)*, last accessed 26.11.2018, URL: http://clic.cern/.

[2] F. Bordry et al., *Machine Parameters and Projected Luminosity Performance of Proposed Future Colliders at CERN* (2018), arXiv: 1810.13022 [physics.acc-ph].

[3] ILC Parameters Joint Working Group, *ILC Staging and Running Scenarios, ILC-NOTE-2015-066*, 2015.

[4] P. Burrows et al., eds., *Updated baseline for a staged Compact Linear Collider, CERN-2016-004*, CERN, 2016.

[5] H. Abramowicz et al., CLICdp, *Higgs physics at the CLIC electron-positron linear collider*, Eur. Phys. J. **C77** (2017) 475, DOI: 10.1140/epjc/s10052-017-4968-5, arXiv: 1608.07538 [hep-ex].

[6] J. Ellis et al., *Dimension-6 Operator Analysis of the CLIC Sensitivity to New Physics*, JHEP **05** (2017) 096, DOI: 10.1007/JHEP05(2017)096, arXiv: 1701.04804 [hep-ph].

[7] H. Abramowicz et al., CLICdp, *Top-quark physics at the CLIC electron-positron linear collider* (2018), arXiv: 1807.02441 [hep-ex].

[8] The ATLAS Collaboration, *Projections for measurements of Higgs boson signal strengths and coupling parameters with the ATLAS detector at a HL-LHC, ATL-PHYS-PUB-2014-016*, 2014.